Published in final edited form as:
J Nat Prod. 2012 April 27; 75(4): 707–715. doi:10.1021/np2009994.

Waikialoid A Suppresses Hyphal Morphogenesis and Inhibits Biofilm Development in Pathogenic *Candida albicans*

Xiaoru Wang[†,‡], **Jianlan You**[†,‡], **Jarrod B. King**[†], **Douglas R. Powell**[§], and **Robert H. Cichewicz**[*,†,⊥]

Natural Products Discovery Group, Department of Chemistry and Biochemistry, Stephenson Life Sciences Research Center 101 Stephenson Parkway, Room 1000, University of Oklahoma, Norman, Oklahoma, 73019-5251, USA.Ecology and Evolutionary Biology Program, University of Oklahoma, Norman, Oklahoma, 73019-5251, USA

Abstract

A chemically prolific strain of *Aspergillus* was isolated from a soil sample collected near Waikiki Beach, Honolulu, Hawaii. The fungus produced several secondary metabolites that were purified and placed in our natural products library, which was later screened for substances capable of inhibiting biofilm formation by *Candida albicans*. It was determined that one of the secondary metabolites from the Hawaiian fungal isolate, a new complex prenylated indole alkaloid named waikialoid A (**1**), inhibited biofilm formation with an IC_{50} value of 1.4 μM. Another structurally unrelated, presumably polyketide metabolite, waikialide A (**15**), also inhibited *C. albicans* biofilm formation, but was much less potent (IC_{50} value of 32.4 μM). Microscopy studies revealed that compound **1** also inhibited *C. albicans* hyphal morphogenesis. While metabolite **1** appears ineffective at disrupting preformed biofilms, the accumulated data indicate that the new compound may exert its activity against *C. ablicans* during the early stages of surface colonization involving cell adherence, hyphal development, and/or biofilm assembly. Unlike some other stephacidin/notoamide compounds, metabolite **1** was not cytotoxic to fungi or human cells (up to 200 μM), which makes this an intriguing model compound for studying the adjunctive use of biofilm inhibitors in combination with standard antifungal antibiotics.

During the period of February 2009 to October 2011, our research group prepared extracts from just over two thousand fungal isolates originating from three environmentally disparate regions: Alaska, Hawaii, and Oklahoma. Many of the fungal extracts were subsequently screened by LC-ESIMS leading us to classify a selection of the isolates as 'metabolically talented'[1] or 'chemically productive'[2] in reference to their capacities to generate multiple secondary metabolites (for our purposes, we define secondary metabolites as compounds with masses of ~300–1,200 Da that elute from C18 with ~25–85% methanol). From our perspective, extracts containing natural products that fulfill these simple criteria represent potentially valuable sources of drug-like substance and our group is actively engaged in building a modest library of compounds meeting these benchmarks. The functions of the

[*]Corresponding Author: rhcichewicz@ou.edu. Tel: 405-325-6969. Fax: 405-325-6111.
[†]Natural Products Discovery Group, Department of Chemistry and Biochemistry.
[‡]These authors contributed equally to this work.
[§]Department of Chemistry and Biochemistry.
[⊥]Ecology and Evolutionary Biology Program.

ASSOCIATED CONTENT

Supporting Information

NMR (^{1}H and ^{13}C NMR, HSQC, HMBC, COSY, ROESY and NOESY) data for compounds **1**, **14**, **15**, and **16**. CD spectra for compounds **1**, **14**, and **15**. Structures of all secondary metabolites isolated from the Hawaiian *Aspergillus* sp. isolate, associated schemes, tables, and additional bioassay data. This information is available free of charge via the Internet at http://pubs.acs.org.

pure compound library are two-fold: first, it provides a unique chemical resource for bioactive compound discovery that complements our extensive collection of >4,000 microbial-derived crude extracts; and second, it serves as an improved tool for vetting new in-house bioassays prior to screening against crude extracts and fractions.

One of the new biological screens we recently introduced to our lab was designed to identify compounds that inhibit biofilm formation by the pathogenic fungus *Candida albicans.* *Candida* spp. are widely recognized as the single most common source of opportunistic mycoses throughout the world [3–6] with an estimated annual financial burden topping $1 billion in the United States alone.[7] Infections caused by *Candida* spp. are encountered with growing frequency among several patient populations including infants, the elderly, immunocompromised individuals, diabetics, patients receiving oncological treatments, and others.[7] An important feature linked to the propensity of many *Candida* spp. to cause serious infections is their capabilities of generating biofilms. *Candida* biofilms demonstrate remarkable versatility in their abilities to grow on a variety of surfaces including human tissues and implanted devices.[8, 9] Biofilms are thought to play key roles in enhancing morbidity and mortality associated with *Candida* infections since biofilm matrices severely reduce the penetrance of antifungal therapeutics into cells.[8] Moreover, *Candida* biofilms serve as favorable substrates that harbor other pathogens and encourage the expansive growth of polymicrobial (mixed bacterial and fungal) communities.[10, 11] *Candida* biofilms have recently been linked to the emergence of highly drug-resistant persister cell populations, which are purported to be major contributors to infection relapses following the cessation of standard courses of antifungal therapeutics.[12, 13]

In this report, we focus on the preparation of purified natural products from a metabolically-talented *Aspergillus* sp. The fungus was isolated from a soil sample collected in the summer of 2009 near Waikiki Beach, Honolulu, Hawaii. Compounds from the fungus were deposited in our secondary-metabolite library and later screened in our biofilm inhibition assay. As a result of the library screening, several bioactive compounds emerged that inhibited *C. albicans* biofilm-formation. One of the especially noteworthy inhibitors we encountered was obtained from a Hawaiian *Aspergillus* sp. isolate. The compound was found to be a new complex prenylated indole alkaloid that we have named waikialoid A (**1**). To the best of our knowledge, metabolite **1** is among the most potent inhibitors of fungal biofilm formation reported to date.

RESULTS AND DISCUSSION

Structure Characterization of Secondary Metabolites from the Hawaiian *Aspergillus* sp. Isolate

LC-ESIMS examination of the organic extract from the Hawaiian *Aspergillus* sp. isolate demonstrated that this fungal strain was capable of generating many putative secondary metabolites with masses between ~400–900 Da. Prior to scale-up fermentation, further tests were performed on this fungus to compare the effects of different fermentation conditions and growth-medium additives (i.e., the chemical epigenetic modifier[14] suberoylanilide hydroxamic acid at 400, 800, and 1,000 μM[1], as well as 3.5% NaCl) on secondary metabolite production. These experiments provided a revealing set of LC-ESIMS profiles (Supporting Information, Figure S1) confirming that the Hawaiian fungal isolate was capable of generating a diverse assemblage of natural products. Scale-up liquid-state and static cultures of the fungus provided sufficient material that enabled us to purify and promptly dereplicate (by HRESIMS, specific rotation, and ^{1}H and ^{13}C NMR) several components including notoamide B (**2**),[15] sclerotiamide (**3**),[16] notoamide F (**4**),[17] notoamide R (**5**),[18] stephacidin A (**6**),[19] CJ-17665 (also known as avrainvillamide) (**7**),[20] circumdatin C (**8**),[21] circumdatin F (**9**),[22] two diketopiperazines (**10** and **11**),[23] flavacol (**12**),[24, 25] and 3-

isobutyl-6-(1-hydroxyl-2-methylpropyl)-2(1*H*)-pyrazinone (**13**)[24] (Supporting Information, Scheme S1). Four additional metabolites were also purified (**1**, **14–16**) that could not be dereplicated, which led us to thoroughly investigate and characterize their respective structures.

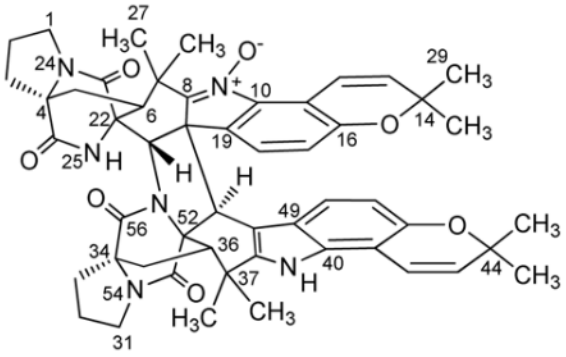

1

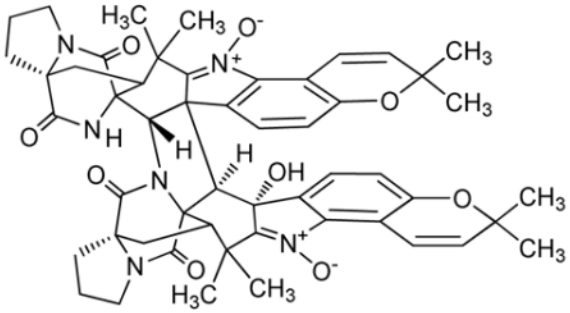

14

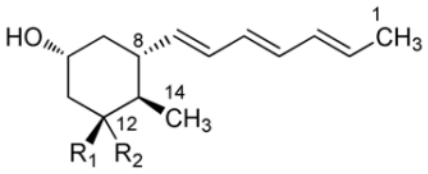

15 $R_1 = R_2 = O$
16 $R_1 = H$, $R_2 = OH$

HRESIMS of purified **1** yielded an adduct ion that was consistent with a molecular formula of $C_{52}H_{54}N_6O_7$. This necessitated that compound **1** possessed 29 degrees of unsaturation. Inspection of the ^1H NMR spectrum of **1** provided a series of proton resonances that were consistent with other compounds in the stephacidin/notoamide family of prenylated indole alkaloid natural products; however, the molecular formula we proposed for **1** was approximately twice the size expected for the majority of metabolites in this series. These data alerted us to a previous report by Cian-Cutrone et al. describing stephacidin B (**17**),[19] which had been shown to be an unusual asymmetric dimerization product of CJ-17665 (**7**) (Supporting Information, Scheme S1).[26] Although a large proportion of the proton and carbon resonance for **1** matched those reported for **17**, the loss of one oxygen atom in the molecular formula of **1** necessitated that the two compounds were different.

Examination of the ^{1}H NMR resonances for the new metabolite (Table 1) revealed that **17** contained a single amide proton (δ_H 7.76, NH-25)[26] and a signal for the *N*-hydroxylamine hydroxyl group (δ_H 10.74, OH-62),[26] whereas **1** possessed two different downfield exchangeable proton singlets (δ_H 7.58 and 7.44) (Table 1). This led us to scrutinize the oxidation state of the N-9 and N-39 nitrogen atoms in **1** since reduction of either the nitrone or *N*-hydroxylamine, respectively, in **17** could have contributed to the loss of one oxygen atom with the concomitant introduction of a new exchangeable amine proton. Examination of the ^{1}H-^{13}C HSQC and ^{1}H-^{13}C HMBC results for **1** (Table 1) provided strong evidence that the N-9 nitrone remained intact, while N-39 was reduced from an *N*-hydroxylamine to an amine. Although other subtle changes in the chemical shifts of carbon atoms near the presumed indole amine provided further evidence in support of this hypothesis, additional data were required to resolve the structure of **1**.

Single-crystal X-ray diffraction was used to confirm the proposed structure of **1**. A concentrated solution of **1** in MeOH (held at 4 °C for ~2 weeks) provided colorless prism-shaped crystals suitable for analysis. The X-ray diffraction data for **1** showed that the new metabolite was an asymmetric pseudo-dimer similar to **17** (Figure 1). In agreement with our NMR-based structure proposal, the N-39 *N*-hydroxylamine in **17** was replaced by an amine in **1**. The absolute configuration of **1** was determined by refinement of the Flack parameter[27] as 4*S*,6*S*,20*S*,21*S*,22*R*,34*S*,36*S*,51*R*,52*R*. In contrast to **17**, which has been reported to degrade in several organic solvents,[19, 26, 28] compound **1** was very stable for days in MeOH and varying H_2O-MeOH mixtures, $CHCl_3$, CH_2Cl_2, and EtOAc. Moreover, **1** was readily observed by LC-MS in crude organic extracts prepared from the Hawaiian *Aspergillus* sp. isolate (Supporting Information, Figure S1), which suggested that this compound may not be an artifact of the isolation process as had been proposed for **17**.[26]

The HRESIMS of the second new metabolite, waikialoid B (**14**), provided a *m/z* that corresponded to a molecular formula of $C_{52}H_{54}N_6O_9$, which represented 29 degrees of unsaturation. Examination of the ^{1}H NMR data (Table 1) established that **14** was structurally related to **1**. In contrast to the seven oxygen atoms in **1**, compound **14** possessed nine oxygens. Several of the carbon resonances in proximity to N-39 were shifted downfield (Table 1), which indicated where one of the new oxygen atoms was likely bonded. Based on the ^{1}H-^{13}C HSQC and ^{1}H-^{13}C HMBC data (Table 1), we rationalized that the N-39 amine in **1** was converted to a nitrone. The downfield shift of C-50 in **14** (δ_C 76.9) could be explained if this carbon was attached to a hydroxyl oxygen; the location of the hydroxyl group was confirmed based on $^{2-3}J_{H\text{-}C}$ couplings observed from OH-62 to C-49, C-50, and C-51 (Table 1).

No suitable crystals of **14** could be generated for single-crystal X-ray diffraction analysis. However, comparisons of the ^{1}H-^{1}H NOESY data for **1** and ^{1}H-^{1}H ROESY data for **14** (Supporting Information, Figures S8 and S16, respectively) revealed strong similarities between the two compounds suggesting a shared relative configuration for both metabolites (4*S**,6*S**,20*S**,21*S**,22*R**,34*S**,36*S**,51*R**,52*R**). One exception was the set of ROESY correlations arising from the additional OH-62 hydroxyl group in **14**. Analysis of the ROE crosspeaks from OH-62 to H-27, H-51, and H-57 enabled us to propose an *R** configuration for C-50. In light of the likely shared biogenic origins for **1** and **14**, as well as the decidedly similar Cotton effects observed in their respective UV–CD spectra ($\Delta\varepsilon$ values for **1** were +29.2 at 231 nm, −82.7 at 254 nm, and −14.4 at 311 nm compared to +16.3 at 226 nm, −18.2 at 243 nm, −8.7 at 320 nm for **14**; Supporting Information Figure S10 and S18, respectively), we propose that the absolute configuration of metabolite **14** is 4*S*,6*S*,20*S*,21*S*, 22*R*,34*S*,36*S*,50*R*,51*R*,52*R*.

Waikialides A (**15**) and B (**16**) were purified from liquid-state cultures of the Hawaiian *Aspergillus* sp. isolate. The molecular formula of compound **15** was determined to be $C_{14}H_{20}O_2$ by HRESIMS indicating five degrees of unsaturation. Analysis of the ^{13}C NMR spectrum (Table 2) provided evidence for six olefinic carbons at δ_C 130.5, 133.2, 133.6, 131.7, 133.0, 136.4. A combination of ^1H-^1H COSY, ^1H-^{13}C HSQC, and ^1H-^{13}C HMBC (Table 2) supported a partial structure for **15** in which the six olefinic carbons formed a conjugated polyene tail (C-2 though C-7) that terminated with an allylic methyl group (C-1). In view of the constraints imposed by the proposed molecular formula, chemical shifts of the unassigned proton and carbon resonances, as well as the presence of a single downfield carbonyl (&*delta;*$_C$ 211.7), we determined that the remaining degree of unsaturation could be accounted for by a monocyle. Constructing this portion of **15** was largely achieved based on the first-order ($^{2-3}J_{H\text{-}H}$) splitting patterns in the 1H NMR spectrum, as well as ^{13}C NMR shift data (Table 2). With three of the remaining hydrogen atoms accounted for by a methyl doublet (δ_H 0.93, J = 6.7 Hz, H-14), and one hydrogen not accounted for in the ^1H NMR data due to deuterium exchange with CD_3OD, a tri-substituted cyclohexanone seemed to be the only feasible substructure for the remaining portion of **15**. The ^1H-^{13}C HMBC data enabled us to construct a hydroxymethylcyclohexanone that was substituted at C-8 by the aforementioned polyene tail. Vicinal $^3J_{H\text{-}H}$ couplings and ^1H-^1H NOESY data (Figure 2A) were instrumental in proposing the 8*S**,10*R**,13*R** relative configuration for **15**. A crystal of **15** was obtained upon slow evaporation from MeOH, which served to corroborate the proposed planar structure and relative configuration of **15** (Supporting Information, Figure S27).

The absolute configuration of **15** was assessed by the octant rule[29] and Mosher ester method.[30] The UV–CD spectrum of **15** exhibited a strong negative Cotton effect at 290 nm due to the n → π* transition of the cyclohexanone carbonyl. By examining which octants the majority of the 8*S*,10*R*,13*R* and 8*R*,10*S*,13*S* enantiomers occupied (the 'negative' rear upper-left octant and 'positive' rear upper-right octant, respectively), we determined that the observed negative Cotton effect (Supporting Information, Figure S28) could only be obtained with the 8*S*,10*R*,13*R* enantiomer. This conclusion was substantiated by results from the Mosher ester experiment in which analysis of the C-10 MTPA ester derivatives **15a** and **15b** supported a 10*R* configuration (Figure 2B).

Waikialide B (**16**) possessed a molecular formula of $C_{14}H_{22}O_2$ as determined by HRESIMS. The loss of one degree of unsaturation in **16** compared to **15** was readily explained upon examination of the ^{13}C NMR data, which revealed that the carbonyl was absent; while a new carbon resonance at δ_C 72.8 supported the presence of a hydroxyl group at the C-10 position. ^1H-^1H COSY, ^1H-^{13}C HSQC, and ^1H-^{13}C HMBC correlation data indicated that the remaining portion of **16** was the same as **15**. Likewise, ^1H-^1H NOESY data demonstrated that the relative 8*S**,10*R**,13*R** configuration of these stereogenic centers was the same as **15**. With these asymmetric carbon atoms accounted for, a prominent NOE enhancement from H-12 (δ_H 3.90) to H-9b (δ_H 1.88) became instrumental in securing a 12*R** configuration for C-12. In light of the presumed similar biosynthetic origins for metabolites **15** and **16**, we propose that the absolute configuration of **16** is 8*S*,10*R*,12*R*,13*R*. It is of interest to note that the waikialides bear considerable resemblance to the diastereomeric natural product 2,3-didehydropalitantin, which was reported from a fungal epiphyte (*Paraphaeosphaeria* sp.).[31]

Assessment of the *C. albicans* Biofilm Inhibition by Purified Metabolites

Purified compounds were tested for their abilities to inhibit both cell viability and biofilm formation of *C. albicans*. None of the 15 metabolites from the Hawaiian *Aspergillus* sp. isolate inhibited *C. albicans* cell viability at concentrations up to 200 μM. In contrast,

compound **1** demonstrated dose-dependent activity in the biofilm inhibition assay with an IC_{50} value of 1.4 ± 0.2 μM (Table 3). This is in sharp contrast to the meager activity afforded by the widely investigated positive control farnesol,[32] which did not impede cell survival, but had an IC_{50} value of 128.6 ± 2.6 μM for biofilm inhibition. Compound **15** also afforded modest inhibition of biofilm formation with an IC_{50} value of 32.4 ± 2.0 μM. Three additional metabolites, **7**, **14**, and **6**, were also detected that weakly inhibited *C. albicans* biofilm formation with IC_{50} values of 43.3 ± 3.5, 46.3 ± 1.6, and 55.2 ± 2.4 μM, respectively (Table 3).

The effects of metabolites **1** and **15** on *C. albicans* hyphae formation were evaluated by phase contrast microscopy. Hyphae formation is an important step in *C. albicans* virulence that marks the transition from initial surface colonization to invasive growth into the underlying matrix.[33–35] Both metabolites **1** and **15** inhibited *C. albicans* hyphae formation in a dose dependent manner (Figure 3 and Supporting Information, Figure S41). Whereas vehicle-treated *C. albicans* cells were observed to form germ tubes at 2.5 h, hyphae at 6 h, and mature biofilms at 24 h post inoculation, cells treated with **1** or **15** did not form germ tubes or hyphae by 6 h and exhibited severely truncated hyphae at 24 h (Supporting Information, Figure S41).

Compound **1** was further evaluated in a time-of-addition study to determine when during the process of biofilm formation the inhibitory effects of the new metabolite were being manifested. The effectiveness of **1** at inhibiting *C. albicans* biofilm formation showed a strong dependence on the time of drug addition (Figure 4). Whereas early time points displayed a small, but steady loss in the effectiveness of **1** at blocking biofilm generation, the later time points (6 and 8 h) exhibited marked drops in the ability of **1** to suppress biofilm formation. Taken together, these data suggest that **1** is likely not effective at inhibiting or disrupting preformed biofilms, but instead exerts its activity against *C. ablicans* during the early stages of surface colonization involving cell adherence, hyphal development, and/or biofilm assembly.

Although the inability of **1** to disrupt established biofilms may limit the potential *in vivo* applications of this metabolite, it is notable that **1** was not toxic to mammalian cells (MIA PACA-2 cell line) at concentrations up to 200 μM (this was rather unexpected since some stephacidins/notoamides are potent human cell toxins; we did observe that **7** and **14** were toxic to MIAPACA-2 cells with IC_{50} values of 11.3 and 8.2 μM, respectively). In light of these results, **1** may have value for exploring in animal model systems since many questions remain concerning the predicted *in vivo* therapeutic utility of inhibitors that selectively and non-lethally block biofilm formation and hyphae development. Several studies have convincingly demonstrated that both biofilm formation and hyphal morphogenesis are important factors intimately associated with drug resistance[36–38] and virulence,[34, 39, 40] respectively, in *C. albicans*. Therefore, both drug resistance traits and virulence factors have been proposed as novel high-value targets for suppressing microbial infections.[40–42] Compounds inhibiting these features are thought to evade the rapid evolution of resistance, since unlike fungicidal antibiotics, they do not pose a lethal, selective threat to microorganisms.[40] Therefore, compound **1** and other secondary metabolites emerging from our *C. albicans* biofilm inhibition screening program hold considerable promise for designing bioactive lead molecules that may function as adjunctive agents in concert with antibiotics.

EXPERIMENTAL SECTION

General Experimental Procedures

Melting points were obtained on a Mel-Temp capillary melting point apparatus. Optical rotation measurements were determined on a Rudolph Research Autopol III automatic polarimeter. UV data were obtained on Hewlett Packard 8452A diode array spectrometer. UV–CD spectra were measured on an AVIV circular dichroism spectrometer model 202-01. IR spectra were measured on A2 Technology Nano FTIR and Bruker Vector 22 FTIR spectrometers. NMR data were obtained on Varian VNMR spectrometers (400 and 500 MHz for ^{1}H, 100 and 125 MHz for ^{13}C) with broad band and triple resonance probes at 20 ± 0.5 °C. Electrospray-ionization mass spectrometry data were collected on an Agilent 6538 high-mass-resolution QTOF mass spectrometer. LC-ESIMS data were obtained using a Thermo-Finnigan Surveyor LC system and Finnigan LCQ Deca mass analyzer. Crude extracts were separated on a Biotage Isolera chromatography system. The HPLC system utilized SCL-10A VP pumps and system controller with a Gemini 5 μm C_{18} column (110 Å, 250 × 21.2 mm, flow rates of 1 to 10 mL/min). X-ray diffraction data for compound **1** were collected on a Bruker APEX II CCD system equipped with a Cu ImuS micro-focus source with Quazar MX optics (λ = 1.54178 Å). X-ray data for compound **15** were collected using a diffractometer with a Bruker APEX CCD area detector and graphite-monochromated Mo K radiation (λ = 0.71073 Å). All solvents were of ACS grade or better.

Organism Collection, Identification, and Culture Methods

An ~1 g portion of a sandy-loam soil sample collected 50 m inland from Waikiki Beach (Honolulu, Hawaii) in July, 2010 was placed in sterile H_2O (10 mL) and diluted 10- and 100-fold. Aliquots (300 μL) of the soil suspensions were spread over the surfaces of 10 cm diameter Petri plates containing Czapek agar with chloramphenicol (100 mg/L). Plates were maintained at 25 °C while exposed to light cycles consisting of 16 h light/8 h dark for four weeks. Colonies were selected from the plates and transferred to fresh Petri plates containing Czapek agar with chloramphenicol (100 mg/L). This process was repeated for each isolate until pure fungal cultures (judged by fungi that presented patterns of color, growth rate, and morphology that were uniform across an entire colony) were established. Pure isolates were transferred to new Petri plates containing Czapek agar (without chloramphenicol) and after 2–3 weeks of incubation at 25 °C, pieces of the agar with mycelia (~0.5 cm^2) were cut and placed in cryogenic storage tubes with sterile glycerol-H_2O (15:85). The tubes were then stored at −80 °C until the fungus was needed for scale-up studies. The fungus investigated in this study was identified as an *Aspergillus* sp. based on sequence analysis of its large-ribosomal-subunit ITS1 region of the rDNA gene. The sequence of the isolate (GenBank accession JQ693975; Supporting Information, Table S3) was compared by BLAST analysis to sequences publicly available through the NCBI database.

For the static preparative-scale culture, fungal mycelia and spores were inoculated into 50 mL potato-dextrose media and grown for one week at 25 °C on an orbital shaker (125 rpm). The cellular material was placed in a sterile Falcon tube and mixed by vortexing for several minutes to create a uniform fungal cell/spore suspension. For the static cultures, aliquots (500 μL) of the fungal suspension were used to inoculate 110 Erlenmeyer flasks (1 L) containing autoclaved medium (0.1 g rice, 0.1 g oatmeal, 0.1 g cornmeal, 0.32 g nutrient broth, ~0.5 g vermiculite, and 50 mL of deionized H_2O; with or without the epigenetic modifier suberoylanilide hydroxamic acid). Culture vessels were maintained on the bench-top at 25 °C for 21 days. For the liquid-state preparative fermentation cultures, aliquots (500 mL) of the fungal suspension were used to inoculate 12 L portions of sterilized potato-dextrose broth in a 20 L fermentor maintained under constant aeration with ~20 L/min of

filtered air with stirring at 200 rpm (Nalgene culture vessel with BioTech mixer). The culture was fermented at 25 °C for 14 days.

Preparative-Scale Cultures, Extraction, and Compound Purification

The scale-up static cultures were extracted overnight with ethyl acetate and the organic layer was removed under vacuum. The resulting organic extract was separated over silica gel on the Isolera MPLC system (mobile phase 1:1 hexane-CH_2Cl_2 to 100% CH_2Cl_2 over 8 min, held at 100% CH_2Cl_2 for 8 min, 100% CH_2Cl_2 to 1:5 MeOH-CH_2Cl_2 over 20 min, and 1:5 MeOH-CH_2Cl_2 to 100% MeOH in 8 min), which yielded four fractions containing compounds for purification. Fraction Fr2 (500 mg, eluted with ~20% CH_2Cl_2 in MeOH) was subjected to preparative HPLC (mobile phase 40% to 100% MeOH in H_2O). This yielded sub-fractions Fr11-14 (~80% MeOH), which were subjected to semi-preparative HPLC to obtain **1** (4 mg), **2** (1 mg), **3** (1.8 mg), **4** (20 mg), **5** (1 mg), **6** (1 mg), **7** (1 mg), **10** (2 mg), **11** (0.3 mg), **12** (13 mg), **13** (2.2 mg), and **14** (1 mg).

The scale-up liquid-state cultures were extracted 3× with ethyl acetate (1:1, vol:vol). The organic layers were retained and the solvent removed under vacuum. The organic extract was separated over silica gel on an Isolera MPLC system (mobile phase 1:1 hexane-CH_2Cl_2 to 100% CH_2Cl_2 over 8 min, held at 100% CH_2Cl_2 for 8 min, 100% CH_2Cl_2 to 1:5 MeOH-CH_2Cl_2 over 20 min, and 1:5 MeOH-CH_2Cl_2 to 100% MeOH in 8 min). The ~15% CH_2Cl_2 in MeOH fraction (660 mg) was subjected to further silica gel MPLC chromotography with 100% CH_2Cl_2 to 1:1 MeOH-CH_2Cl_2. The sub-fraction eluting with ~12% MeOH (320 mg) was subjected to prep-HPLC (mobile phase 30% to 100% MeOH in water) to provide compounds **8** (10 mg), **9** (12 mg), **15** (9.5 mg) and **16** (61.8 mg).

Waikialoid A (1)—clear prism-shaped crystals (MeOH); mp: 174–176 °C, $[\alpha]^{21}_D$ −12.0 (*c* 0. 15, MeOH); UV (MeOH) λ_{max} (log ε) 206 (4.99), 264 (4.75), 302 (4.39) nm; CD (MeOH; $\Delta\varepsilon$) 231(+29.2), 254 (−82.7), 311 (−14.4); IR ν_{max} 1680, 2980, 3120, 3320, 3490 cm^{-1}; ^1H and ^{13}C NMR data, see Table 1; HRESIMS *m/z* 875.4119 $[M + H]^+$ (calcd for $C_{52}H_{55}N_6O_7$, 875.4132).

Waikialoid B (14)—yellow, amorphous solid; $[\alpha]^{21}_D$ 28.5 (*c* 0.035, MeOH); UV (MeOH) λ_{max} (log ε) 206 (4.74), 264 (4.29) nm; CD (MeOH; $\Delta\varepsilon$) 226 (+16.3), 243 (−18.2), 320 (−8.7); IR ν_{max} 1590, 2920, 2980, 3390 cm^{-1}; ^1H and ^{13}C NMR data, see Table 1; HRESIMS *m/z* 905.3827 $[M - H]^-$ (calcd for $C_{52}H_{53}N_6O_9$, 905.3874).

Waikialide A (15)—white, crystalline solid; mp: 115–117 °C, $[\alpha]^{21}_D$ 11.4 (*c* 0.035, MeOH); UV (MeOH) λ_{max} (log ε) 202 (4.38), 266 (4.81) nm; CD (MeOH; $\Delta\varepsilon$) 266 (10.9), 293(−9.9); IR ν_{max} 1690, 2910, 2920, 2950, 2980, 3000, 3430 cm^{-1}; ^1H and ^{13}C NMR data, see Table 2; HRESIMS *m/z* 243.1378 (calcd for $C_{14}H_{20}O_2Na$, 243.1361).

Waikialide B (16)—white, amorphous solid; $[\alpha]^{21}_D$ 97.1 (*c* 0.175, MeOH); UV (MeOH) λ_{max} (log ε) 202 (4.43), 268 (3.93) nm; IR (KBr) ν_{max} 2910, 3400 cm^{-1}; ^1H and ^{13}C NMR data, see Table 2; HRESIMS *m/z* 221.1543 $[M - H]^-$ (calcd for $C_{14}H_{21}O_2$, 221.1542).

Preparation of Mosher Ester Derivatives 15a and 15b

Compound **15** was transferred into two NMR tubes (0.25 mg each, 0.0011 mmol) and dried under vacuum. The samples in each tube were treated with dry pyridine (0.4 mL each) and 0.5μL (0.00267 mmol) of (*S*)-(+)-*R*-methoxy-*R*-(trifluoromethyl)-phenylacetyl chloride (MTPA chloride) or (*R*)-(−)-*R*-methoxy-*R*-(trifluoromethyl) phenylacetyl chloride reagent. The mixture was reacted at room temperature for 4 h and its completion was confirmed by ^1H-NMR. This provided the two derivatives **15a** and **15b**. ^1H-NMR spectra of both

derivatives were collected in pyridine-d_5, along with ^{1}H-^{1}H COSY data, which were used to assign the proton resonances.

***S*-MPTA ester of derivative of 15 (15a)—**^{1}H NMR (500 MHz, pyridine-d$_5$) δ_H 6.12–6.36 (4H, m, H-3, H-4, H-5, H-6), 5.74 (1H, dd, *J* = 7.1, 14.4 Hz, H-2), 5.44–5.57 (2H, m, H-3, H-10), 3.11 (1H, d, *J* = 10.8 Hz, H-11), 2.79 (1H, t, *J* = 12.2 Hz, H-11), 2.20–2.34 (2H, m, H-8, H-13), 2.06–2.16 (1H, m, H-9),1.76–1.87 (1H, m, H-9), 1.69 (3H, d, *J* = 6.4 Hz, H-1), 1.06 (3H, d, *J* = 6.4 Hz, H-14).

***R*-MPTA ester of derivative of 15 (15b)—**^{1}H NMR (500 MHz, pyridine-d$_5$) δ_H 6.13–6.39 (4H, m, H-3, H-4, H-5, H-6), 5.69–5.80 (1H, m, H-2), 5.45–5.59 (2H, m, H-3, H-10), 3.04 (1H, ddd, *J* = 2.0, 5.1, 13.0 Hz, H-11), 2.65 (1H, t, *J* = 12.0 Hz, H-11), 2.32 (1H, dt, *J* = 5.1, 12.2 Hz, H-9), 2.25 (1H, dt, *J* = 6.4, 12.1 Hz, H-13), 2.13 (1H, tdd, *J* = 2.9, 8.7, 11.8 Hz, H-8), 1.86–1.96 (1H, m, H-9), 1.69 (3H, dd, *J* = 1.2, 6.6 Hz, H-1), 1.07 (3H, d, *J* = 6.4 Hz, H-14).

X-ray Crystal Structure Analysis

X-ray diffraction data of **1** were collected on a Bruker APEX II CCD system equipped with a Cu ImuS micro-focus source with Quazar MX optics. A total of 67703 data were measured in the range $3.54 < \theta < 67.16°$ using ϕ and ω oscillation frames. The data were merged to form a set of 7859 independent data with R(int) = 0.0272 and a coverage of 97.6 %. A total of 635 parameters were refined against 21 restraints and 7859 data to give wR(F^2) = 0.0845 and S = 1.005 for weights of $w = 1/[\sigma^2 (F^2) + (0.0530\ P)^2 + 0.9000\ P]$, where $P = [F_0^2 + 2F_c^2]/3$. The final R(F) was 0.0316 for the 7855 observed, [$F > 4\sigma(F)$], data. The calculated minimum and maximum transmission coefficients (based on crystal size) are 0.6520 and 0.8418. The structure was solved by direct methods and refined by full-matrix least-squares methods on F^2. The goodness-of-fit was 1.005. The largest shift/s.u. was 0.033 in the final refinement cycle. The final difference map had maxima and minima of 0.343 and −0.281 e/Å3. On the basis of the final model, the calculated density was 1.309 g/cm3 and F(000), 984 e-. The X-ray crystallographic data for **1** has been deposited with the Cambridge Crystallographic Data Center under accession number CCDC864505. This data can be accessed free of charge at http://www.ccdc.cam.ac.uk/.

X-ray diffraction data of **15** were collected on a Bruker APEX CCD area detector and graphite-monochromated Mo K radiation (= 0.71073 Å). A total of 4,287 data were measured in the range $2.36 < \theta < 22.99°$ using ϕ and ω oscillation frames, the data were corrected for absorption by semi-epirical methods giving minimum and maximum transmission factors of 0.9613 and 0.9970. The data were merged to form a set of 1000 independent data with R(int) = 0.1127 and a coverage of 99.8%. The structure was solved by direct methods and refined by full-matrix least-squares methods on F^2. Hydrogen atom positions were initially determined by geometry and refined by a riding model. Non-hydrogen atoms were refined with anisotropic displacement parameters. A total of 150 parameters were refined against one space group restraint and 1,000 data to give wR(F^2)=0.1720 and S=1.051 for weights of $w=1/[\sigma^2(F^2)+(0.0880P)^2+0.4400P]$, where $P=[F_0^2+2F_C^2]/3$. The final R(F) was 0.0710 for the 730 observed, [$F>4\sigma(F)$], data. The largest shift/s.u. was 0.000 in the final refinement cycle. The final difference map had maxima and minima of 0.227 and −0.257 e/Å3, respectively. The X-ray crystallographic data for **15** has been deposited with the Cambridge Crystallographic Data Center under accession number CCDC864506. This data can be accessed free of charge at http://www.ccdc.cam.ac.uk/.

Assay for Growth Inhibition and Biofilm Formation

The effects of compounds on the growth of *C. albicans* DAY185 were tested using the method described in the NCCLS 2002 CLSI M27-A2 guidelines.[43] The biofilm assay was performed as described [44] with the following modifications. *C. albicans* DAY185 was cultured in BHI medium (brain heart infusion, Becton Dickinson and Company) at 37 °C overnight. The cells were pelleted by centrifugation, washed with sterile PBS (phosphate-buffered saline, pH 7.4, EMD Chemicals, Inc.), and resuspended in RPMI 1640 medium (Sigma Chemical Corporation) buffered to pH 7.0 with MOPS (0.165 M, Sigma). Test compounds were prepared in DMSO at stock concentrations of 20 mM before being serially diluted in RPMI 1640 plus MOPS medium for testing. Farnesol was used as a positive control for assessing biofilm inhibition.[45] Aliquots of yeast suspension (100 μL containing 2.5×10^3 cells/mL) were added to the medium containing the diluted compounds or DMSO (1% by vol.) before being transferred to 96-well microplates (Costar 3370, Corning, Inc.). After 48 h of incubation at 37 °C, the viability of the yeast were measured using the XTT assay.[46] In brief, yeast cells were treated with 0.1 mg/mL XTT at 37 °C for 1 h. The absorbance was taken at 490 nm using a microplate reader (Infinite M200, Tecan Group Ltd.). The minimum inhibitory concentration (MIC) for growth was defined as the lowest antifungal concentrations that caused ≥80% reduction in the metabolic activity.

For measuring biofilm formation, the medium was aspirated and the wells were washed twice with sterile PBS to remove non-adherent cells. Fresh medium (100 μL RPMI 1640 plus MOPS) was then added back to each well. The formation of biofilms was measured using the XTT assay.[46] All experiments were performed in triplicate on three separate occasions. The 50% inhibitory concentration value (IC_{50}) for biofilm inhibition was calculated using GraphPad Prism software.

Hyphae Formation Assay

C. albicans DAY185 was grown in BHI medium at 37 °C overnight. The cells were pelleted, washed, and suspended in sterile PBS (pH 7.4, EMD). Cells were seeded in 96-well plates at 1×10^6 cells/well and incubated at 37 °C for 1 h. Wells were washed twice with sterile PBS to remove non-adherent cells. RPMI 1640 containing 2% glucose and compounds (**1**, **15**, or farnesol – positive control[45]) in DMSO (1% by vol.) was added to each well and the plates were incubated at 37 °C for 24 h. Hyphae formation was monitored with a phase contrast microscope at 2.5, 6 and 24 h.[44]

Biofilm Time of Addition Assay

Using the techniques described above for the biofilm formation inhibition assay, compound **1** (from 100 μM to 0.2 μM) was added at −0.5, 0, 2, 4, 6, and 8 h after seeding *C. albicans* DAY185 cells in a 96-well microplate. At 48 h after inoculation, the wells were washed twice with PBS and the amount of biofilm formation in each well was determined by XTT assay.[47] The 50% inhibitory concentration (IC_{50}) value for biofilm inhibition was calculated using GraphPad Prism software. All experiments were performed in triplicate on three separate occasions.

Cell Cytotoxicity Assay

The mammalian cell cytotoxicity screening assay was performed by adding 10^4 MIA PaCa-2 cells per well of a 96-well plate and allowing the cells to attach overnight at 37 °C in a humidified incubator with a 5% CO_2 atmosphere. The next day, test compounds in DMSO were added to the wells (final DMSO concentration 1% by vol.) and incubated for 24 h. Cell viability was determined by MTT assay.

Supplementary Material

Refer to Web version on PubMed Central for supplementary material.

Acknowledgments

We wish to acknowledge the National Institutes of Health (1RO1GM092219 and 1RO1AI085161) for financial support. The X-ray diffractometer was purchased through a grant from the NSF (CHE-0130835). We gratefully acknowledge the help of C. Campana for collection the X-ray diffraction data for **1**. We also thank C. A. Kumamoto (Tufts University, USA) and A. Mitchell (Carnegie Mellon University, USA) for the supplying the *C. albicans* DAY185 strain.

References

1. Williams RB, Henrikson JC, Hoover AR, Lee AE, Cichewicz RH. Org Biomol Chem. 2008; 6:1895–1897. [PubMed: 18480899]
2. Janso JE, Carter GT. Appl Environ Microbiol. 2010; 76(13):4377–4386. [PubMed: 20472734]
3. Lass-Flörl C. Mycoses. 2009; 52:197–205. [PubMed: 19391253]
4. Ruan SY, Hsueh PR. J Formos Med Assoc. 2009; 108:443–451. [PubMed: 19515624]
5. Playford EG, Nimmo GR, Tilse M, Sorrell TC. J Hosp Infect. 2010; 76:46–51. [PubMed: 20382444]
6. Falagas ME, Roussos N, Vardakas KZ. Int J Infec Dis. 2010; 14:954–966.
7. Pfaller MA, Diekema DJ. Clin Microbiol Rev. 2007; 20:133–163. [PubMed: 17223626]
8. Julia LD. Trends Microbiol. 2003; 11:30–36. [PubMed: 12526852]
9. Harriott MM, Lilly EA, Rodriguez TE, Fidel PL, Noverr MC. Microbiology. 2010; 156:3635–3644. [PubMed: 20705667]
10. Dongari-Bagtzoglou A, Kashleva H, Dwivedi P, Diaz P, Vasilakos J. PLoS ONE. 2009; 4:e7967. [PubMed: 19956771]
11. Harriott MM, Noverr MC. Trends Microbiol. 2011; 19:557–563. [PubMed: 21855346]
12. LaFleur MD, Qi Q, Lewis K. Antimicrob Agents Chemother. 2010; 54:39–44. [PubMed: 19841146]
13. LaFleur MD, Kumamoto CA, Lewis K. Antimicrob Agents Chemother. 2006; 50:3839–3846. [PubMed: 16923951]
14. Cichewicz RH. Nat Prod Rep. 2010; 27:11–22. [PubMed: 20024091]
15. Kato H, Yoshida T, Tokue T, Nojiri Y, Hirota H, Ohta T, Williams RM, Tsukamoto S. Angew Chem Int Ed. 2007; 46:2254–2256.
16. Whyte AC, Gloer JB, Wicklow DT, Dowd PF. J Nat Prod. 1996; 59:1093–1095. [PubMed: 8946752]
17. Tsukamoto S, Kato H, Samizo M, Nojiri Y, Onuki H, Hirota H, Ohta T. J Nat Prod. 2008; 71:2064–2067. [PubMed: 19053517]
18. Tsukamoto S, Umaoka H, Yoshikawa K, Ikeda T, Hirota H. J Nat Prod. 2010; 73:1438–1440. [PubMed: 20795742]
19. Qian-Cutrone J, Huang S, Shu YZ, Vyas D, Fairchild C, Menendez A, Krampitz K, Dalterio R, Klohr SE, Gao Q. J Am Chem Soc. 2002; 124:14556–14557. [PubMed: 12465964]
20. Sugie Y, Hirai H, Inagaki T, Ishiguro M, Kim YJ, Kojima Y, Sakakibara T, Sakemi S, Sugiura A, Suzuki Y, Brennan L, Duignan J, Huang LH, Sutcliffe J, Kojima N. J Antibiot. 2001; 54:911–916. [PubMed: 11827033]
21. Rahbaek L, Breinholt J, Frisvad JC, Christophersen C. J Org Chem. 1999; 64:1689–1692. [PubMed: 11674237]
22. Rahbaek L, Breinholt J, Circumdatins DEF. J Nat Prod. 1999; 62:904–905. [PubMed: 10395516]
23. Furtado NAJC, Pupo MT, Carvalho I, Campo VL, Duarte MCT, Bastos JK. J Braz Chem Soc. 2005; 16:1448–1453.
24. Li HJ, Cai YT, Chen YY, Lam CK, Lan WJ. Chem Res Chin Univ. 2010; 26:415–419.
25. Dunn G, Newbold GT, Spring FS. J Chem Soc. 1949:2586–2587.

26. Herzon SB, Myers AG. J Am Chem Soc. 2005; 127:5342–5344. [PubMed: 15826171]
27. Flack H. Acta Crystallogr A. 1983; 39:876–881.
28. Wulff JE, Herzon SB, Siegrist R, Myers AG. J Am Chem Soc. 2007; 129:4898–4899. [PubMed: 17397160]
29. Murphy WS. J Chem Edu. 1975; 52:774.
30. Hoye TR, Jeffrey CS, Shao F. Nat Protoc. 2007; 2:2451–2458. [PubMed: 17947986]
31. Lee HB, Oh H. Bull Korean Chem Soc. 2006; 27:779–782.
32. Ramage G, Saville SP, Wickes BL, López-Ribot JL. Appl Environ Microbiol. 2002; 68:5459–5463. [PubMed: 12406738]
33. Kumamoto CA, Vinces MD. Cell Microbiol. 2005; 7:1546–1554. [PubMed: 16207242]
34. Brand A. Int J Microbiol. 2012; 2012:517529. [PubMed: 22121367]
35. Sudbery PE. Nat Rev Microbiol. 2011; 9:737–748. [PubMed: 21844880]
36. Finkel JS, Mitchell AP. Nat Rev Microbiol. 2011; 9:109–118. [PubMed: 21189476]
37. Uppuluri P, Srinivasan A, Ramasubramanian A, Lopez-Ribot JL. Antimicrob Agents Chemother. 2011; 55:3591–3593. [PubMed: 21518839]
38. Al-Fattani MA, Douglas LJ. J Med Microbiol. 2006; 55:999–1008. [PubMed: 16849719]
39. Pukkila-Worley R, Peleg AY, Tampakakis E, Mylonakis E. Eukaryot Cell. 2009; 8:1750–1758. [PubMed: 19666778]
40. Shareck J, Belhumeur P. Eukaryot Cell. 2011; 10:1004–1012. [PubMed: 21642508]
41. Gauwerky K, Borelli C, Korting HC. Drug Discov Today. 2009; 14:214–222. [PubMed: 19152839]
42. Alksne LE, Projan SJ. Curr Opin in Biotechnol. 2000; 11:625–636.
43. Clinical and Laboratory Standards Institute. Reference Method for Broth Dilution Antifungal Susceptibility Testing of Yeasts - Approved Standard (CLSI document M27-A3). 3. 2008.
44. Chandra J, Mukherjee PK, Ghannoum MA. Nat Protoc. 2008; 3:1909–1924. [PubMed: 19180075]
45. Deveau A, Hogan DA. Methods Mol Biol. 2011; 692:219–233. [PubMed: 21031315]
46. Nett JE, Cain MT, Crawford K, Andes DR. J Clin Microbiol. 2011; 49:1426–1433. [PubMed: 21227984]
47. Zhang Y, Cai C, Yang Y, Weng L, Wang L. J Med Microbiol. 2011; 60:1643–1650. [PubMed: 21778264]

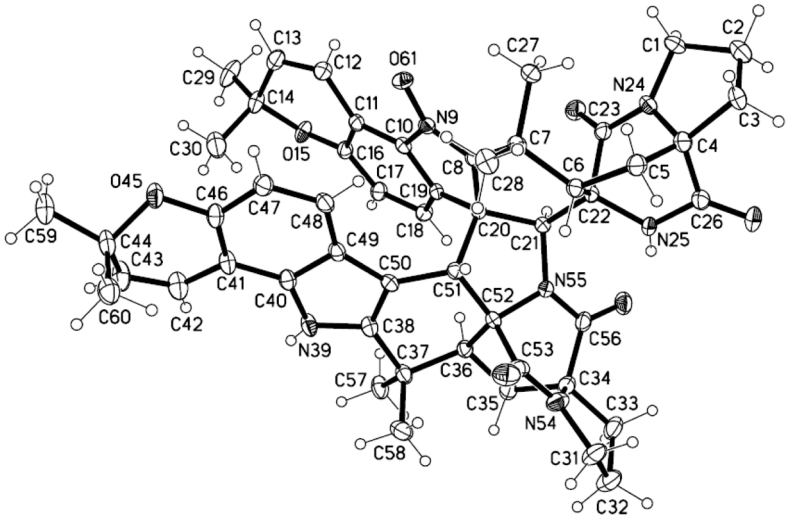

Figure 1.
ORTEP structure generated from the X-ray diffraction data for a single crystal of **1** that was obtained from MeOH.

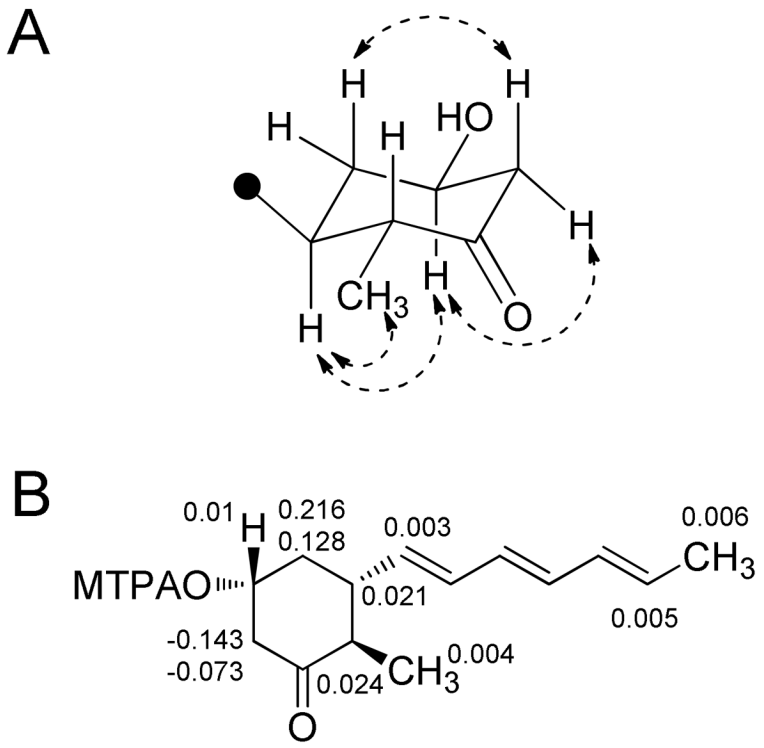

Figure 2.
A) ^{1}H-^{1}H NOESY correlations (dashed double-headed arrows) used to corroborate the relative configuration of the cyclohexanone substructure in metabolite **15**. B) Calculated $\delta_H(S) - \delta_H(R) = \Delta\delta_{SR}$ values for the Mosher ester derivatives **15a** and **15b**.

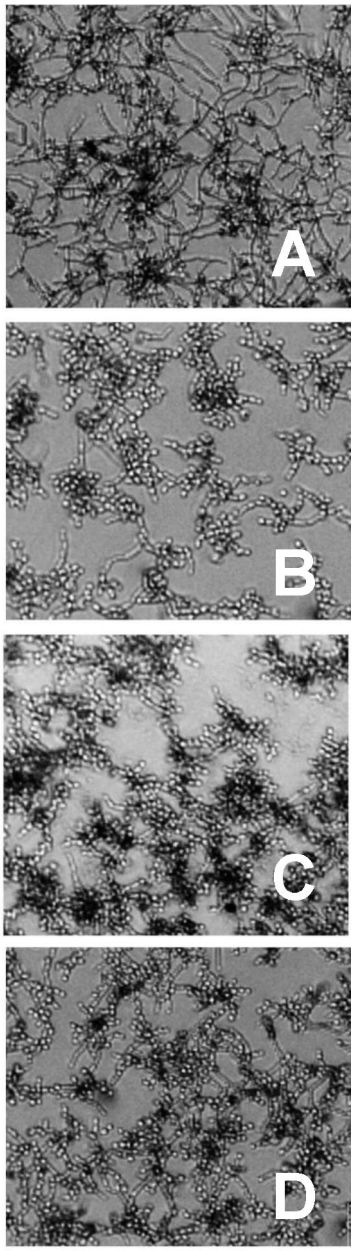

Figure 3.
Testing the impact of purified secondary metabolites on *C. albicans* DAY185 hyphae formation. Freshly inoculated cells were treated with A) vehicle only (DMSO), B) farnesol (50 μM), C) waikialoid A (**1**) (50 μM), D) waikialide A (**15**) (50 μM), and incubated for 6 h prior to visualization by phase contrast microscopy (magnification ×200). Note the significant network of hyphal growth in the vehicle control, which is significantly reduced or absent from nearly all cells in the treatment groups. The effects of addition doses of these compounds are shown in the Supporting Information, Figure S41.

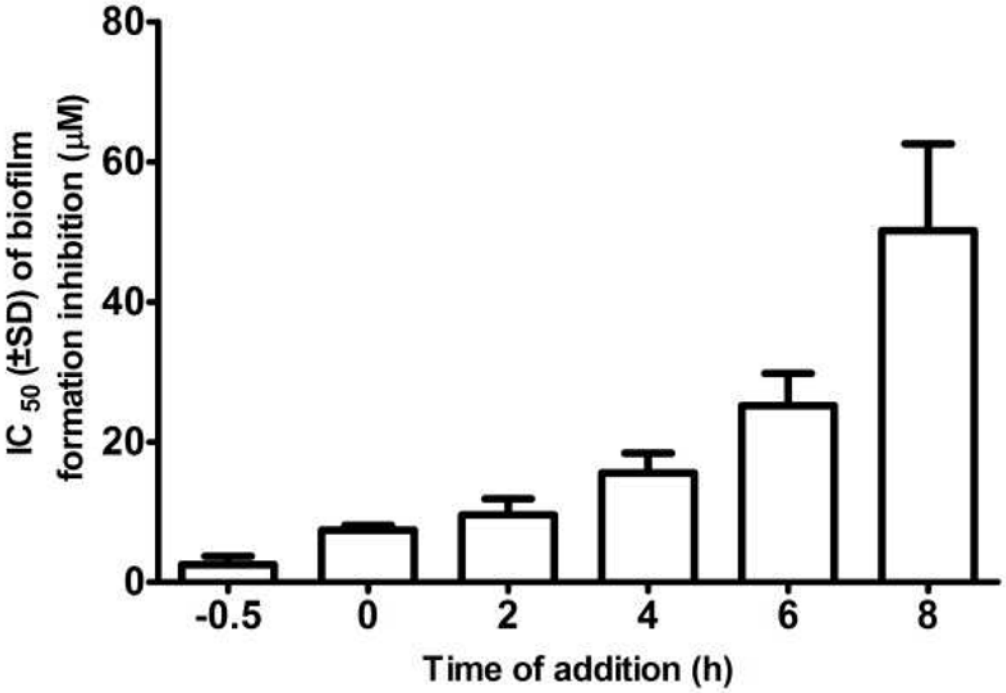

Figure 4.

Time-of-addition study of compound **1**. The compound was added to each well (doses ranging from 100 μM to 0.2 μM) at designated time points immediately before (−0.5 h) or after (0, 2, 4, 6, and 8 h) inoculation of *C. albicans* DAY185 into microplates. Following 48 h of incubation, the wells were washed twice with PBS and the extent of biofilm formation determined by XTT assay. The 50% inhibitory concentration (IC_{50}) value for biofilm inhibition was calculated using GraphPad Prism software. The experiment was replicated three times with each treatment tested in triplicate during each trial. The effects of single doses of compound **1** at these time points are shown in the Supporting Information, Figures S42 and S43. The difference in the relative potency of **1** at the −0.5 and 0 h addition time points is due to the delay in solubilization of **1** in aqueous medium at room temperature (25 °C).

J Nat Prod. Author manuscript; available in PMC 2013 April 27.

Table 1

^{1}H (500 MHz), ^{13}C (100 MHz), and ^{1}H-^{13}C NMR data for **1** and **15** ($CDCl_3$)

	waikialoid A (1)			waikialoid B (15)		
position	**δ_C, type**	**δ_H, mult. (*J* in Hz)**	**HMBC (H→C)**	**δ_C[a], type**	**δ_H, mult. (*J* in Hz)**	**HMBC(H→C)**
1a	44.2, CH_2	3.29, td (7.2, 11.6)	C-2,3,4	43.8, CH_2	3.19, m	
1b		3.47, m			3.41, m	
2	24.8, CH_2	2.00, m	C-1,3	24.6, CH_2	1.98, m	C-26,37
					2.22, m	C-4,7,26
3a	29.4, CH_2	1.83, m	C-1,2,4,5,26	29.1, CH_2	1.81, m	C-4,26
3b		2.76, td (6.5, 12.8)			2.75, m	C-4,6,26
4	65.8, qC			65.5, qC		
5	28.6, CH_2	2.16, m	C-4,6,7,26	28.7, CH_2	2.12, m	C-5,26
					2.20, m	C-4,26
6	43.6, CH	3.00, m	C-4,5,7,23,27,28	43.0, CH	2.74, m	C-22,23,27,28
7	38.1, qC			38.0, qC		
8	151.3, qC			148.5, qC		
10	140.0, qC			140.9, qC		
11	113.0, qC			112.6, qC		
12	116.7, CH	7.56, d (10.5)	C-10,13,14,16	116.9, CH	7.34, d (10.3)	C-14,16
13	131.7, CH	5.52, d (10.5)	C-11,14	131.8, CH	5.54, d (10.2)	C-11,14
14	76.4, qC			76.3, qC		
16	153.6, qC			154.6, qC		
17	115.0, CH	6.44, d (8.3)	C-11,16,19	115.4, CH	6.98, d (8.4)	C-10,16,20
18	120.7, CH	6.89, d (8.3)	C-10,11,16	120.6, CH	6.70, d (8.3)	C-11,16,19
19	129.7, qC			124.0, qC		
20	61.8, qC			58.7, qC		
21	58.2, CH	5.55, s	C-6,19,20,22,23,52	59.7, CH	5.25, s	C-6,19,20,22,23,51,52
22	64.6, qC			64.8, qC		
23	167.1, qC			166.2, qC		
25-NH		7.44, s	C-4,6,21,26		7.78, s	C-22

	waikialoid A (1)			waikialoid B (15)		
position	**δ_C, type**	**δ_H, mult. (*J* in Hz)**	**HMBC (H→C)**	**δ_C[a], type**	**δ_H, mult. (*J* in Hz)**	**HMBC(H→C)**
26	174.2, qC			173.7, qC		
27	17.0, CH_3	1.68, s	C-7,8,28	18.2, CH_3	1.60, s	C-6,7,8,28
28	26.6, CH_3	1.83, s	C-6,7,8,27	27.5, CH_3	1.76, s	C-6,7,8,27
29	27.4, CH_3	1.15, s	C-13,14,30	27.6, CH_3	1.26, s	C-13,14,30
30	27.4, CH_3	1.28, s	C-13,14,29	28.9, CH_3	1.47, s	C-13,14,29
31a	44.6, CH_2	3.62, m	C-31,32,34	45.0, CH_2	3.73, m	
31b		3.47, m				
32	25.0, CH_2	2.11, m	C-31,33,34	28.7, CH_2	2.12, m	C-34,56
					2.20, m	C-56
33a	29.9, CH_2	1.99, m	C-32,33,34,56	29.5, CH_2	2.09, m	C-34,35,56
33b		2.94, m			2.95, m	C-34,56
34	68.8, qC			68.5, qC		
35a	30.9, CH_2	2.02, m	C-36,37,52,56	31.7, CH_2	1.99	C-34
35b		2.42, dd (10.5, 12.5)			2.44, dd (9.8, 12.8	
36	46.9, CH	3.08, dd (6.7, 10.3)	C-35,37,52,53,57,58	51.2, CH	3.12, dd (8.5, 17.5)	C-35,37,52.53
37	34.2, qC			37.0, qC		
38	141.4, qC			146.8, qC		
39		7.58, s	C-38,40,49,50			
40	132.7, qC			139.1, qC		
41	104.6, qC			112.6, qC		
42	117.0, CH	6.40, d (9.8)	C-41,44,46	116.9, CH	7.48, d (10.3)	C-44,46
43	129.7, CH	5.58, d (9.8)	C-41,44	131.4, CH	5.61, d (10.3)	C-41,44
44	75.6, qC			76.3, qC		
46	148.8, qC			154.9, qC		
47	111.0, CH	6.64, d (8.3)	C-41,46,48	118.4, CH	6.78, d (8.3)	C-41,46,49
48	120.1, CH	7.14, d (8.8)	C-40,46,49,50	122.8, CH	7.06, d (8.3)	C-40,46,50
49	120.4, qC			124.0, qC		
50	103.5, qC			76.9, qC		
51	43.4, CH	5.14, s	C-,8,10,19,20,36,50,52,53	52.2, CH	4.46, s	C-20,36,53,8,49,50,52

J Nat Prod. Author manuscript; available in PMC 2013 April 27.

	waikialoid A (1)			waikialoid B (15)		
position	**δ_C, type**	**δ_H, mult. (*J* in Hz)**	**HMBC (H→C)**	**δ_C[a], type**	**δ_H, mult. (*J* in Hz)**	**HMBC(H→C)**
52	70.4, qC			71.1, qC		
53	168.8, qC			169.5, qC		
56	174.3, qC			174.0, qC		
57	22.4, CH_3	1.02, s	C-36,37,38,58	27.4, CH_3	1.22, s	C-36,37,38,58
58	27.5, CH_3	1.26, s	C-36, 37,38,57	26.4, CH_3	1.74, s	C-36,37,38,57
59	27.4, CH_3	1.37, s	C-43,44,60	19.5, CH_3	1.25, s	C-43,44,60
60	27.4, CH_3	1.39, s	C-43,44,59	28.8, CH_3	1.47, s	C-43,44,59
62-OH					6.46, s	C-49,50,51

[a]: δ_C was assigned based on $^1H \rightarrow ^{13}C$ HSQC and HMBC NMR data

Table 2

^{1}H (400 MHz), ^{13}C (100 MHz), and ^{1}H-^{13}C HMBC NMR data for **15** and **16** (CD_3OD)

	waikialide A (15)			waikialide B (16)		
position	**δ_C, type**	**δ_H, mult. (*J* in Hz)**	**HMBC(H→C)**	**δ_C, type**	**δ_H, mult. (*J* in Hz)**	**HMBC(H→C)**
1	18.5, CH_3	1.78, d (6.8)	C-2,3	18.6, CH_3	1.77, d (6.7)	C-2,3
2	130.5, CH	5.73, qd (14.3, 6.8)	C-1,3	129.8, CH	5.66, m	C-3,1
3	133.2, CH	6.13, m		131.8, CH	6.06, m	
4	133.6, CH	6.13, m		131.8, CH	6.06, m	
5	131.7, CH	6.13, m		132.6, CH	6.06, m	
6	133.0, CH	6.13, m		133.3, CH	6.06, m	
7	136.4, CH	5.55, dd (13.7, 9.0)	C-5,6	138.8, CH	5.46, dd (13.7, 9.0)	C-6,8
8	46.0, CH	1.95, dddd (9.0, 11.3, 13.0, 3.8)[a]	C-6,7,13,9,14	42.2, CH	2.11, m	C-6,7
9a	42.9, CH_2	1.67, ddd (11.3, 11.3, 11.6)[a]	C-7,8,10,11,13	43.4, CH_2	1.16, ddd (11.6, 10.0, 11.6) [a]	C-7,8,10
9b		2.08, ddddd (11.3, 3.8, 3.9, 2.2,2.2)[a]	C-11		1.88, dddd (12.1, 2.0, 3.5, 4.0) [a]	C-8,10
10	69.7, CH	3.78, dddd (11.6, 3.9, 4.2, 11.4)[a]	C-8,9	66.3, CH	3.95, m	C-9
11a	52.0, CH_2	2.45, ddd (11.2, 11.4, 2.5)[a]	C-10,9,12	43.5, CH_2	1.39, ddd (12.0, 11.7, 2.7)[a]	C-10,12
11b		2.65, ddd (11.2, 4.8, 2.5)[a]	C-9,10,12,13		2.16, m	C-9,10
12	211.7, qC			72.8, CH	3.90, m	C-10,14
13	49.5, CH	2.25, dq (13.0, 6.5)	C-7,8,12,14	41.8, CH	1.28, m	C-14
14	12.6, CH_3	0.93, d (6.7)	C-8,12,13	16.8, CH_3	0.91, d (7.0)	C-12,13

[a]: *J* assignments were confirmed by modeling using ACD predictor software.

J Nat Prod. Author manuscript; available in PMC 2013 April 27.

Table 3

Inhibition of *C. albicans* biofilm formation and cell growth

Compound	IC_{50}[a] of biofilm inhibition (μM)	MIC[b] of growth inhibition (μM)
1	1.4 ± 0.2	>200
2	108.6 ± 3.7	>200
3	93.5 ± 3.6	>200
5	97.3 ± 5.5	>200
6	55.2 ± 2.4	>200
7	43.3 ± 3.5	>200
14	46.3 ± 1.6	>200
15	32.4 ± 2.0	>200
16	97.0 ± 2.1	>200
farnesol	128.6 ± 2.6	>200

[a] IC_{50} expressed as the concentration of compound corresponding to a 50% reduction of *C. albicans* biofilm formation

[b] MIC values were defined as the lowest concentration causing ≥80% reduction in the metabolic activity of *C. albicans* as determined by conversion of XTT to its colored product